Colloid Polym Sci (2005) 284: 1–9
DOI 10.1007/s00396-005-1319-0

ORIGINAL CONTRIBUTION

The influence of oxidative degradation on the preparation of chitosan nanoparticles

A. L. P. Fernandes
W. A. Morais
A. I. B. Santos
A. M. L. de Araújo
D. E. S. dos Santos
D. S. dos Santos
F. J. Pavinatto
O. N. Oliveira Jr.
T. N. C. Dantas
M. R. Pereira
J. L. C. Fonseca

Received: 04 November 2004
Accepted: 13 January 2005
Published online: 11 August 2005

A. L. P. Fernandes · W. A. Morais
A. I. B. Santos · A. M. L. de Araújo
D. E. S. dos Santos · T. N. C. Dantas
M. R. Pereira · J. L. C. Fonseca (✉)
Departamento de Química,
Universidade Federal do Rio Grande
do Norte, C.P. 1662 Lagoa Nova,
Natal 59078-970, Brazil
E-mail: jlcfonseca@uol.com.br
Tel.: +55-84-2153828
Fax: +55-84-2119224

D. S. dos Santos · F. J. Pavinatto
O. N. Oliveira Jr.
Instituto de Física de São Carlos,
Universidade de São Paulo,
Av. Trabalhador São Carlense, 400,
C.P. 369 São Carlos 13566-590, Brazil

Abstract Chitosan nanoparticles were obtained via ionic crosslinking by using the sulfate ion. Chitosan molecular weight was varied by oxidative degradation of the chitosan β-glycoside bond, the molecular weight being indirectly monitored as the chitosan solution reduced viscosity at a fixed polymer concentration. The dependence between some physical properties of the resultant dispersions (turbidity, viscosity, zeta potential, and sedimentation column profile) and reduced viscosity was established. Atomic force microscopy images have shown the resultant particles formed to be clusters of chitosan nanoparticles with a diameter of ca. 70 nm, the interaction between these particles being characterized by FTIR spectroscopy as the result of sulfate bridging. At the end of the paper, the potential of these dispersions for the incorporation of anionic drugs via adsorption was evaluated using a model compound. The resultant dispersions were capable of adsorbing more than 25% of mass of chitosan, being the partition coefficient higher than 3,500.

Keywords Chitosan · Particles · Adsorption · Controlled release

Introduction

Chitosan is a biomaterial derived from the deacetylation of chitin, an abundant biopolymer, present in many crustaceans, insects, and mollusk shells [1]. The versatility of chitosan has been repeatedly reported in the literature: this biopolymer has been used in sensors [2, 3], in hybrid (ceramic/organic) materials [4], as coagulant [5], and heavy metal absorber [6] in water treatment. When in the form of membranes, transport properties of this material are suitable for use with salt solutions [7] as well as drug permeation [8]. The most remarkable characteristic of chitosan is its biocompatibility, which has made this material adequate for use in biomedicine (e.g., in the form of implants [9, 10], artificial skins [11, 12]), controlled drug release (in the form of gels [13], membranes [14], and particulate systems [15–19]).

One of the properties that has attracted attention toward this biopolymer is its mucoadhesivity [20]. When protonated, chitosan can interact with the mucous layer, due to the presence of sialic acid as one of its main components [21]. Since sialic acid is negatively charged, chitosan (which is a cationic polyelectrolyte) electrostatically interacts with this layer, resulting in good adhesion and prolonged residence time in the site of liberation [22, 23]. This property may be used in the liberation of antibiotics to eliminate bacteria that are harmful to the stomach, such as *Helicobacter pylori*, the main agent that provoke ulcers, gastritis and gastric carcinoma [24].

Specifically regarding the preparation of chitosan-based particulate systems, chitosan particles may be obtained using spray-drying methods [25, 26]. These methods involve rater complex steps, using organic solvents, vaporization, and high vacuum: as a consequence, simpler methods have been developed in which chitosan particles are directly obtained from its aqueous solutions by chemical reactions or electrostatic interactions [27]. They may involve covalent crosslinking [28], complexation, and precipitation from aqueous solutions [29]. The simplest and most direct way of obtaining these particles is through the neutralization of the weakly acidic NH_3^+ groups present in the chain, via the addition of NaOH [30]. When in a highly polar environment such as an aqueous solution, as the macromolecule is neutralized, it loses polarity and as a consequence precipitates [31]. Covalent crosslinking is performed via the reaction between non-protonated NH_2 groups and organic compounds such as glutaraldehyde [18, 32]. Covalent crosslinking, however, may introduce two problems: (1) it may restrict the mobility (or, more exactly, the release) of the active substance [33], and (2) non-reacted glutaraldehyde may cause mucosal irritation [34].

Electrolyte-related complexation is a form of circumventing the problem of glutaraldehyde toxicity: electrostatic interactions between protonated amino groups of chitosan (positively charged) and polycharged anions result in a physically equivalent system [35]. Polycharged anions may be in the form of macromolecules, such as poly(acrylic acid) [36], or low molecular weight anions, such as tripolyphosphate (TPP) [17, 37–40] and sulfate [41, 19, 42, 43].

In a previous work, our group has shown the importance of variables such as the use of ultrasonication, content of surfactant and sulfate ions on some properties of chitosan dispersions (turbidty, zeta potential, and dispersion viscosity) [44]. The aim of this work is to show the influence of polyelectrolyte molecular weight on such properties. At the end of this work, the feasibility of using these particulate systems for the incorporation of anionic organic molecules will be investigated: this behavior is related to the incorporation of negatively charged drugs to chitosan particles as well as the adhesion of these very particles to negatively charged surfaces, rich in sialic acid.

Experimental

Acetic acid (PA, Reagen, Brazil), K_2SO_4 (PA, Labsynth, Brazil), the non-ionic surfactant polyoxyethylene-sorbitan monooleate (Tween 80, Sigma, USA, Fig. 1I), methyl orange (VETEC LTDA, Brazil, Fig. 1-II), potassium sulfate (K_2SO_4, VETEC LTDA), and potassium persulfate ($K_2S_2O_8$, VETEC LTDA) were used without further purification. Chitosan was purchased from Polymar (Brazil) and had an 85% degree of deacetylation. The polymer was obtained from shrimp shells and had viscosity average molecular weight, $M_v \approx 2.9\times10^5$ g mol^{-1}, determined using Mark-Howink-Sakurada equation from viscometric data [45], and using a buffer solution of 0.5 M CH_3COOH and 0.2 M CH_3COONa ($K = 3.5\times10^{-4}$ (dL·g^{-1}) (mol·g^{-1})$^{\alpha}$; $\alpha = 0.76$; $[\eta] = (5.0 \pm 0.1)$ dL g^{-1}). All solutions were filtered using a Millipore Millex filter, prior to use. In all experiments, bidistilled water was used.

All experiments were performed at least three times and error propagation of a determined quantity Y, function of other k quantities x_i ($i = 1, 2, 3, ..., k$) was calculated using the following relationship [46]:

$$\Delta Y \leq \sum_{i=1}^{k} \left|\frac{\partial Y}{\partial x_i}\right| \Delta x_i, \quad (1)$$

where ΔY is the propagated error and (associated with the quantity Y) and Δx_i is the error associated with the quantity x_i.

Preparation of dispersions

Chitosan dispersions were prepared by the addition of aqueous K_2SO_4 to chitosan solutions, in the presence of surfactant (Tween 80). An appropriate volume of a K_2SO_4 100 g L^{-1} solution was added at a volume flow rate of 1.5 mL min^{-1} (using a burette) to a 250-mL erlenmeyer containing 100 mL of a 2.5 g L^{-1} chitosan solution (the solvent being aqueous acetic acid at 20 g L^{-1}) and a given amount of surfactant. During the complete addition, the erlenmeyer was immersed in an ultrasonic bath (Transsonic model T460, Germany, tank volume 2.75 L, frequency of operation 45 Hz,

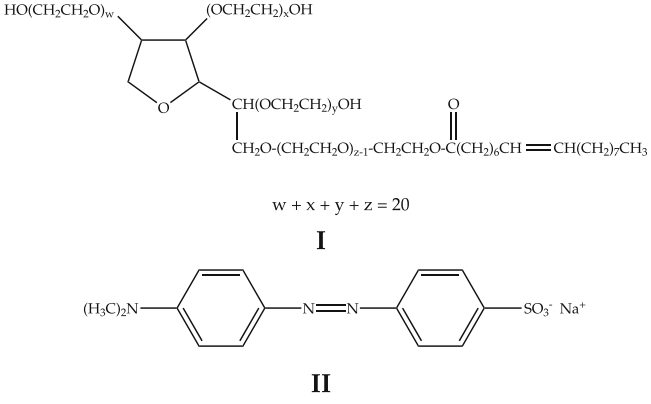

Fig. 1 Chemical structure of nonionic surfactant Tween 80 (I) and the dye methyl orange (II)

power 170 W), at a temperature of 30 °C and mechanically stirred. The stirrer was driven by a servo motor (9V DC, as used in turntables) which had a nominal rotation N of 2,100 rpm. The impeller had a diameter D of 2 cm, so that the resulting nominal Reynolds number was $\mathrm{Re} = DN^2\rho/\mu \approx 2 \cdot (2,100/60)^2 \cdot 1/0.01 \approx 2 \times 10^5$, where $\rho = 1$ g/cm^3 and $\mu = 0.01$ P are, respectively, the approximate density and viscosity of the solutions. The resultant dispersion was withdrawn from the ultrasonic bath after 20 min (this time taking into account the time involved in the addition of the K_2SO_4 solution). In all the experiments, the final concentration of K_2SO_4 (i.e., after the addition was carried out),$C_{K_2SO_4}$, was 0.0058 mol L^{-1} and the final surfactant concentration, C_S, was 10 g L^{-1}. These values were chosen due to results obtained in a previous work [44]: at this sulfate concentration, zeta potential is exactly between the maximum and the minimum obtained in our experiments, and this value of surfactant concentration is exactly between the maximum and the minimum used in the cited work.

Viscometry, turbidimetry and zeta potential analyses were carried out after the dilution of the resultant dispersions to 10% of their initial concentration. This dilution was carried out using a 20 g L^{-1} acetic acid aqueous solution. The variable involved in the preparation of the dispersions was the molecular weight of chitosan (indirectly monitored as the reduced viscosity at a standard concentration). Chitosan with different molecular weights were obtained via oxidative degradation as described in Sect. 2.2.

Chitosan degradation

Chitosan was degraded using the oxidation of the β-glycoside linkage of polysaccharides, a reaction already reported in the literature [47, 48]. The experimental procedure used in these reactions was based on the one used in the analysis of the kinetics of similar oxidative degradation [more specifically, ether linkages of poly(ethylene oxide) by potassium persulfate] [49]. Different amounts of potassium persulfate were added to 2.5 g L^{-1} chitosan solutions. The system was left under stirring, at room temperature, for 24 hours. The used final persulfate concentrations, $C_{K_2S_2O_8}$, were 1.9×10^{-5}, 1.9×10^{-4}, and 1.9×10^{-3} mol L^{-1}. For each resultant solution, the reduced viscosity was determined as described in Sect. 3.

Viscometry

Viscometry of the resultant dispersions was carried out using a Ubbelohde viscometer #0B, previously calibrated with different fluids. When determining the reduced viscosity, η_{red}, it was done as already described in the literature [50, 51]:

$$\eta_{red} = \frac{1}{C_c}\left(\frac{t}{t_0} - 1\right),$$

where t_0 is the efflux time for the solvent, t is the efflux time of the chitosan solution, and C_c is the chitosan concentration. The temperature used in these tests was (30.00 ± 0.05) °C. The solvent efflux time was 198.5 s, so that there was no need for shear rate corrections. When calculating the reduced viscosity, the exact concentration of chitosan was obtained by gravimetry (evaporation of 10 mL of the chitosan at 105 °C, until constant weight).

Atomic force microscopy (AFM)

Atomic force microscopy images were obtained in tapping mode, employing a resonance frequency of approximately 300 kHz, a scan rate of 0.71 Hz, and scan areas of 1 μm^2, using a digital AFM-nanoscope IIIa instrument. The tip used was made of silicon. The particles were separated from the aqueous dispersion using ethyl alcohol, followed by centrifugation at 10,000 rpm for 1 h and deposited on a clean mica surface, prior to analysis.

FTIR spectroscopy

FTIR spectra were carried out using a Thermo Nicolet Nexus 470 spectrometer using disks made of chitosan particles pressed with KBr (these particles were separated from suspension via centrifugation, washed with ethanol and dried at 55 °C until constant mass). The operational parameters were: number of scans, 32; resolution, 4 cm^{-1}. In order to perform comparisons, spectra of the following samples were also carried out—pure chitosan, chitosan with Tween 80, and chitosan particles obtained in a medium with final sulfate concentration of 0.0088 mol L^{-1}. Chitosan with Tween 80 were obtained from thin films made by casting the solutions of chitosan (described in Sect. 2.1), without the addition of sulfate. The resultant films were left in an oven, at 50 °C for 24 h, prior to analysis.

Turbidimetry

Turbidimetry was carried out using a Hach turbidimeter (model 2100P, USA). The instrument was equipped with a tungsten-filament lamp and a 90 ° detector to monitor scattered and transmitted light. According to the man-

ufacturer, the lamp yielded white light with a continuous spectrum. The instrument's microprocessor calculated the ratio of the signals from 90 ° and transmitted light detectors, correcting interferences from color and/or light absorbing materials. All the samples were analyzed immediately after homogeneization (for higher values of turbidity, it slowly decreased with time after about 30 s). All the measurements were taken at room temperature [(25 ± 2) °C].

Electrophoretic mobility and zeta potential measurements

The electrophoretic mobility measurements, μ_E, were carried out using a Zeta-Meter System 3.0+ (Zeta-Meter Inc., USA). Zeta potential, ζ, was calculated from μ_E by employing the Smoluchowski relationship [52]:

$$\zeta = \frac{\mu_E \eta}{\epsilon_0 \epsilon}, \tag{2}$$

where ϵ_0 is the permittivity of vacuum, ϵ is the dielectric constant of water, and η is the viscosity of the medium. All the measurements were taken at room temperature [(25 ± 2) °C].

Sedimentation experiments

A provette was filled with 100 mL of a given dispersion, prepared as described in Sect. 2.1. After 15 days resting at room temperature [$T = (25 \pm 2)$ °C], aliquots of 10 mL were carefully collected (so that there was no development of turbulence) using a volumetric pipette from the upper part of the column to the bottom of it (in this case, with sediment homogeneization). All the aliquots were diluted to one tenth of the initial concentration using a solution of acetic acid 20 g L^{-1}. The turbidity of the diluted aliquots was determined as described in Sect. 2.6. The aliquots were labeled as $n = 1$ (upper part of the column) to $n = 10$ (bottom of the column).

Adsorption isotherms

For these experiments the particles were prepared as described in Sect. 2.1. However, in this specific case, potassium sulfate was added up to the point where turbidity reached a constant value, indicating that all chitosan was ionically crosslinked and precipitated. The resulting dispersion was left resting at room temperature for 1 day. The supernatant was carefully removed using a syringe and the solid particles were washed with water (three times), water/EtOH 1:1 (three times), and water (six times). From this process a slurry consisting of chitosan content, w_c, around 1 wt.% was obtained (chitosan concentration was determined by gravimetry, at 105 °C).

A given mass of chitosan slurry, m_c, was then weighted and mixed with a mass of methyl orange solution, m_d, of density ρ_d, and concentration $C_{d,0}$. After homogenization, systems with different $C_{d,0}$ rested for 5 days in sealed tubes at a temperature of (21 ± 2) °C and pH = 4.2 ± 0.1. After this time the tubes underwent centrifugation at 40,000 rpm, for 1 h, and the concentration of methyl orange in the supernatant phase, C_d, was determined using a UV-visible Cary spectrometer model 1E, at the wavelength of 471 nm, from a previously built calibration curve at the same pH. Since the volume occupied by chitosan is not significant (in terms of overall volume), the total volume of the supernatant may be considered as the sum of the volume of water from the chitosan dispersion, $V_{w,c}$ and the volume of the methyl orange solution, V_d, which may be given as:

$$V = V_{W,c} + V_d = \frac{(1 - w_c)m_c}{\rho_w} + \frac{m_d}{\rho_d} \approx \frac{(1 - w_c)m_c + m_d}{\rho_w}, \tag{3}$$

where ρ_w is the density of water. The mass of methyl orange adsorbed per gram of chitosan, Γ, was calculated as

$$\begin{aligned} \Gamma &= \frac{C_{d,0}(m_d/\rho_d) - C_d(((1 - w_c)m_c + m_d)/\rho_w)}{w_c m_c} \\ &\approx \frac{C_{d,0}m_d - C_d[(1 - w_c)m_c + m_d]}{\rho_w w_c m_c}. \end{aligned} \tag{4}$$

The partition coefficient, K, is defined as the ratio between the concentration of dye in the chitosan particles, $C_{d,c}$, and the concentration of dye in the continuous phase, C_d, and is calculated as

$$K = \frac{C_{d,c}}{C_d} = \frac{\Gamma m_c w_c / V_{c,h}}{C_d} = \frac{\Gamma \rho_{c,h}}{C_d} \Rightarrow \frac{K}{\rho_{c,h}} = \frac{\Gamma}{C_d}, \tag{5}$$

where $V_{c,h}$ is the volume occupied by the hydrated chitosan particles and $\rho_{c,h}$ is the density of the hydrated chitosan particles, which was assumed to be independent of the amount of adsorbed dye.

Results and discussion

Figure 2 shows an AFM image of an ensemble of particles centrifugated from a chitosan dispersion obtained with non-degraded chitosan. One can see that the coagulation process yielded particles composed of chitosan nanoparticles with a "raspberry morphology": this sort of morphology has already been found in polyaniline-based particle systems [53, 54] and was the result of bridging flocculation induced by solubilized segments of the polyelectrolyte, as well as by sulfate

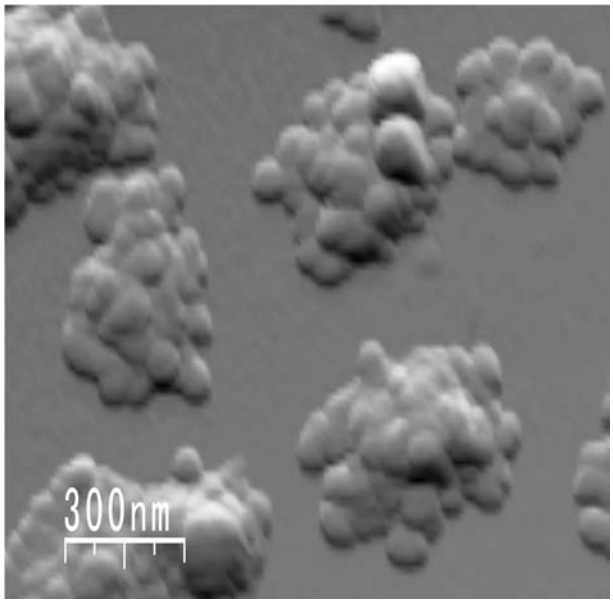

Fig. 2 Atomic force microscopy image of an ensemble of chitosan particles

bridging. The size of the particles in the clusters were around 70 nm.

Figure 3 shows the FTIR spectra of (a) chitosan, (b) chitosan with surfactant, (c, d) chitosan nanoparticles with different sulfate final concentrations (all samples prepared with non degraded chitosan), and (e) pure potassium sulfate. The FTIR spectrum of chitosan showed characteristic peaks of amide groups: amide I and amide II bands at 1,647 and 1,598 cm^{-1}, respectively. The intense band at around 3,420 cm^{-1} should be assigned to the stretching vibration of O–H and/or N–H, as well as to intermolecular hydrogen bonding within the polysaccharide molecules [55]. The absorption bands at 1,154 cm^{-1} (antisymmetric stretching of the C–O–C bridge), 1,078 and 1,031 cm^{-1} (skeletal vibrations involving the C–O stretching) are characteristic of chitosan's saccharide structure [56] . The spectrum of chitosan with surfactant did not present new absorptions since all the groups present in the surfactant are also present in chitosan. On the other hand, as salt concentration increased, the spectra of the nanoparticles underwent an increase in intensity of absorptions coming from the sulfate group: these were at 1,113 cm^{-1} (S–O stretching) and 618 cm^{-1} (SO_4^{2-} bending) [57–59], as can be verified by comparison with the spectrum of pure potassium sulfate. It indicates an increase in ionic crosslinking.

Table 1 shows the relationship between reduced viscosity, η_{red}, and persulfate concentration, $C_{K_2S_2O_8}$, of chitosan solutions after degradation with different amounts of persulfate [chitosan concentration, in a dry basis, was $C_C = (0.200 \pm 0.005)$ g L^{-1}]. The direct determination of chitosan molecular weight from these

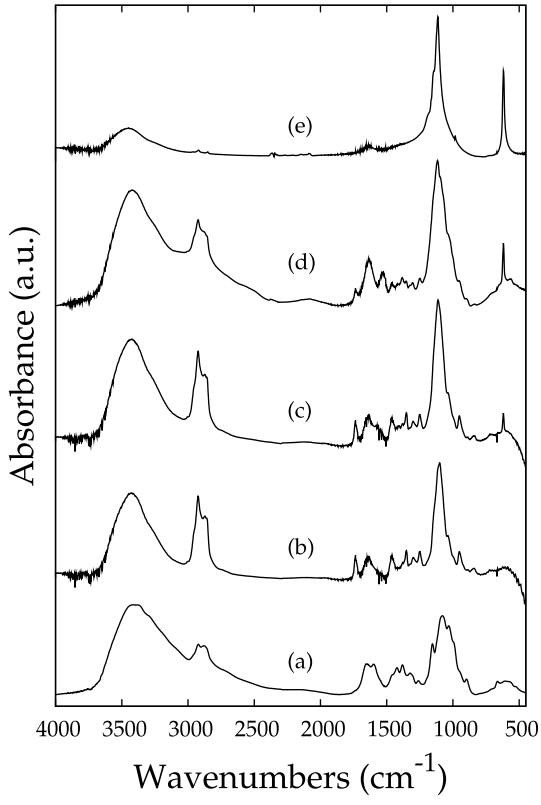

Fig. 3 FTIR spectra of (**a**) pure chitosan, (**b**) chitosan with Tween 80, (**c**) chitosan nanoparticles ($C_{K_2SO_4} = 0.0058$ mol L^{-1}), (d) chitosan nanoparticles ($C_{K_2SO_4} = 0.0088$ mol L^{-1}), and (e) K_2SO_4

Table 1 Reduced viscosity, η_{red}, as a function of persulfate concentration, $C_{K_2S_2O_8}$

$C_{K_2S_2O_8}$ (10^{-3}mol L^{-1})	$[\eta]$ (dL g^{-1})
0	16.0 ± 0.3
0.019	14.3 ± 0.2
0.19	6.3 ± 0.2
1.9	1.3 ± 0.1

data is limited by two experimental circumstances. (1) the solutions were not buffered, so that Huggins equation could not be used due to the polyelectrolyte effect [60]. (2) polymer concentration was certainly above the critical concentration for coil overlapping, $C^* = C_C^*[\eta] \approx 0.8$ [50, 61]; if one has in mind that intrinsic viscosity in acetic acid solution is higher than in the bufffer solution used to determine viscometric molecular weight (polyelectrolyte effect), $C_C[\eta] > 0.2 \times 5 = 1$. Despite these considerations, one can affirm that the decrease in reduced viscosity (at a fixed polymer concentration and solvent system) clearly evidences the decrease in chitosan molecular weight, as the concentration of persulfate was increased. This result is

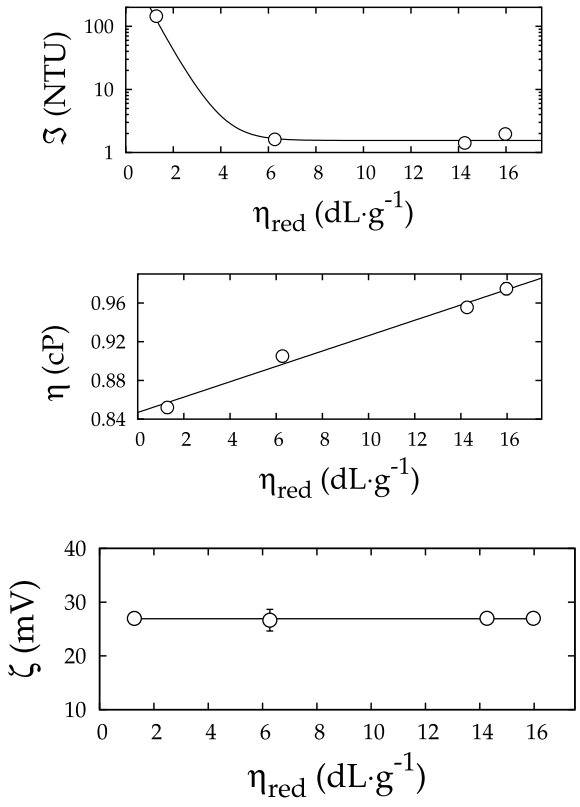

Fig. 4 Turbidity,ϑ, viscosity, η, and zeta potential, ζ, of chitosan dispersion as a function of the reduced viscosity, η_{red}, of the chitosan solution used to prepare it

in agreement with poly(ethylene oxide) oxidative degradation studies already reported in literature by our group [49].

Figure 4 shows how turbidity,ϑ, viscosity, η, and zeta potential, ζ, vary with reduced viscosity, η_{red}. ζ did not change with chitosan molecular weight, which is consistent with the fact that surface charge did not change (since the concentration of sulfate ions was kept constant and persulfate concentration was lower than the sulphate one). The lowest molecular weight chitosan yielded dispersions which were more difficult to visualize in the zetameter, which suggests that as a result of drastic decrease in molecular weight, there was also a pronounced decrease in particle size. The viscosity of the dispersion increased with the increase of molecular weight, indicating higher molecular weight chitosan solubilized in the continuous phase and/or a higher amount of chitosan solubilized in the continuous phase (in a previous work we have shown that viscosity may be used to monitor changes in the dispersing phase, while particle size/concentration effects are more evident by turbidimetry [44]). The decrease of ϑ, as a result of η_{red} increase, indicates that particle formation is favored by lower molecular weights. At a first sight, this is not consistent with the fact that solubility of pure chitosan decreases as molecular weight is increased, as found by Mao et al. [62]. When analyzing polyelectrolyte complexation, however, one must keep in mind that since polymer molecular weight decreases, macromolecular coil dimensions also decrease (with an increase in the number of macromolecular coils). The decrease in coil dimensions would imply a higher fraction of ionizable groups at the outer regions of the polymer coils. Since groups closer to the surface coil are more easily ionizable, the resultant macromolecules will be more charged. More charged molecules offer a higher number of ionic crosslinking points to sulfate ions: this would result in a higher amount of produced particles. Even if ionization degree were the same, smaller coil dimensions would imply relatively more extended polymer conformations; more extended polymer conformations would imply higher surface contact between polymer coils; as a result, a higher occurrence of particles would take place.

Figure 5 shows turbidity as a function of aliquot of sedimentation column for dispersions made from chitosan solutions with different reduced viscosities. As seen before, as the molecular weight of chitosan decreases, turbidity increases, indicating that there is a more intense formation of particles. The presence of a plateau is also evodent between $n=1$ and $n=9$ (for higher molecular weight chitosan dispersions), indicating a constant particle concentration and/or constant particle size (since turbidity depends both in concentration and particle size). Another reason could be the faster kinetics of sedimentation of bigger particles resulting in lower dispersion stability, as already reported in the literature [52]. As molecular weight decreases, this plateau is less defined so that a gradient is developed, which is consistent with a less homogeneous particle size distribution (higher fraction of particles with smaller dimensions) and/or with a higher particle stability. The first hypothesis is strengthened by the fact that zeta potential was independent of chitosan molecular weight (an increase in surface charge would imply higher stability [63], in electrostatic terms). As a consequence, it appears that chitosan molecular weight rules dispersion stability via sedimentation kinetics, while it does not have a decisive influence regarding flocculation of formed particles by electrostatic interactions. Regarding bridging flocculation, however, increase in molecular weight of chitosan solubilized in the continuous phase may have destabilized the dispersions via the adsorption of macromolecules on a higher number of formed particles (by purely electrostatic interactions or hydrogen bonding), as already described in the literatrure for some polyelectrolyte/oxide systems [64].

Figure 6 shows the isotherm of adsorption of methyl orange on the chitosan particles as well as the ratio between the partition coefficient and the hydrated chitosan particle density, $K/\rho_{c,h}$. One can see that the particles

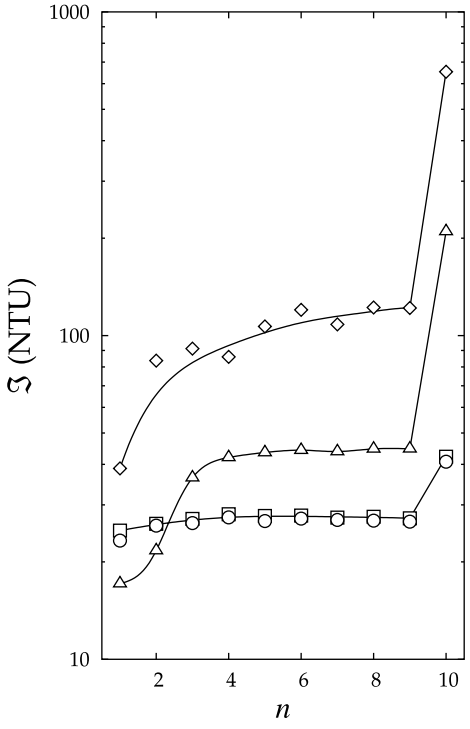

Fig. 5 Turbidity as a function of n for dispersions obtained with chitosan of different molecular weights. *Squares* $\eta_{red} = (16.0 \pm 0.3)$dL g^{-1}. *Circles* $\eta_{red} = (14.3 \pm 0.2)$dL g^{-1}. *Triangles* $\eta_{red} = (6.3 \pm 0.2)$dL g^{-1}. *Diamonds* $\eta_{red} = (1.3 \pm 0.1)$dL g^{-1}

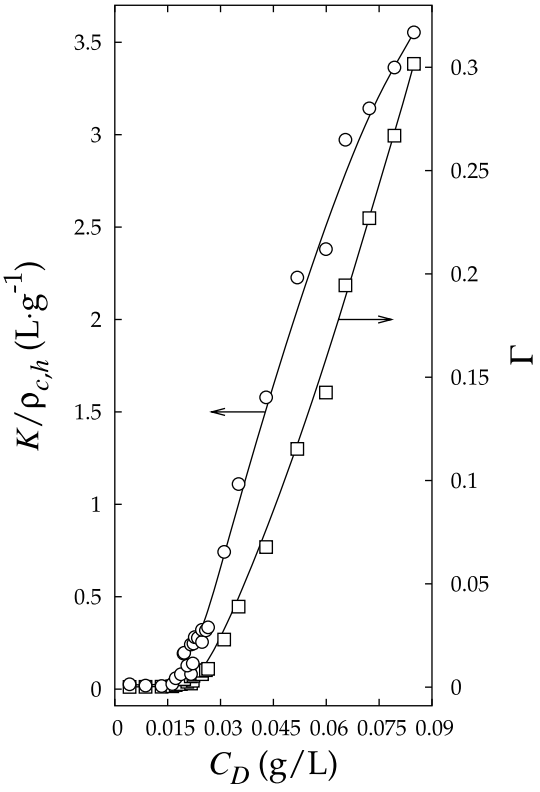

Fig. 6 Adsorption isotherm of methyl orange on chitosan particles. *Squares* Γ. *Circles* $K/\rho_{c,h}$

may be successfully used for the adsorption of anionic molecules. If one has in mind that $\rho_{c,h} > \rho_w \approx 1{,}000$ g L^{-1}, where ρ_w is the density of water, as dye concentration is increased, K reaches values higher than 3,500. This result, as well as the absence of a well defined plateau in the isotherm, may be explained by two hypothesis's, which are depicted in Fig. 7. In the first hypothesis, which is correlated to Scheme 1 of Fig. 7, the adsorption of the monocharged anion would destroy an ionically crosslinked site. This destruction would yield a more opened up particle (probably with a higher porosity), enhancing the adsorption of the dye. The second hypothesis, depicted in Scheme 2 of Fig. 7, relates the adsorption to a possible protonation of the amino groups present in the dye molecules (it is expected that, once protonated, these amino groups would be sterically more available to the adsorption of dye molecules, compared to the original NH_3^+ groups from chitosan). Although these groups are strongly protonated only at pH $\leq$ 3.1 [65] (the pH used in our experiments was 4.2), part of the NH_2 must still be protonated. Some authors have found similar behavior for chitosan particle systems obtained in a wide variety of forms (at some pH's, chitosan was able to incorporate more than 1,000 g of dye per kg of chitosan) [66–69].

Conclusion

Chitosan dispersions obtained via ionic crosslinking by sulfate anion had properties such as viscosity and turbidity highly dependent on the molecular weight of chitosan, while surface charge remained unaltered. Particle sizes were within the nanometric range and, with respect to FTIR spectroscopy, the chemical nature of the particles showed sulfate features that indicated ionic crosslinking. Decrease in chitosan molecular weight increased the yield of particles while, on the other hand, it seemed to decrease particle size. These systems showed themselves as potentially useful for the incorporation of anionic drugs and/or adhesion to negatively charged surfaces where a mucous layer, rich in negatively charged sialic acid, plays an important role.

Acknowledgements The authors thank Brazil's Conselho Nacional de Desenvolvimento Científico e Tecnológico (CNPq), Ministério da Ciência e Tecnologia (MCT), Fundação Coordenação de Aperfeiçoamento de Pessoal de Nível Superior (CAPES), FAPESP, and Pró-Reitoria de Pesquisa e Pós-Graduação da Universidade Federal do Rio Grande do Norte (PROPESQ-UFRN) for financial support during the course of this work.

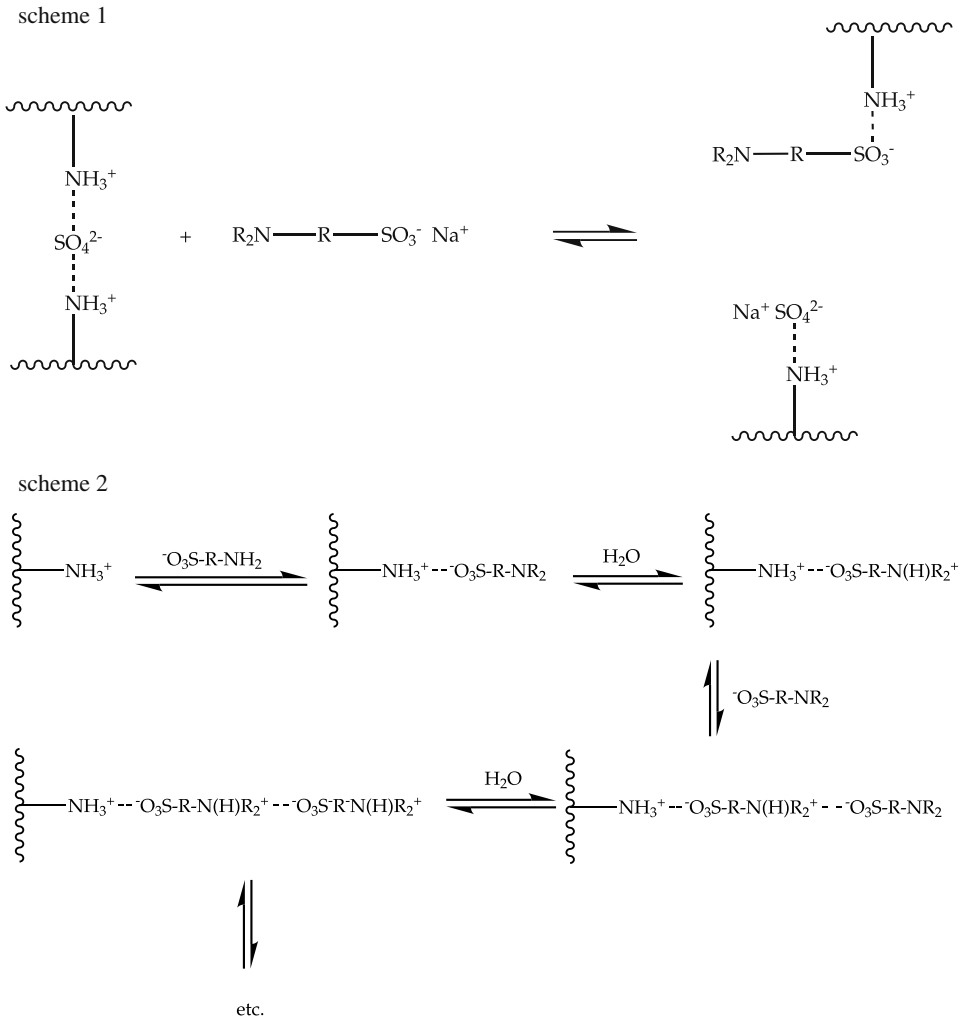

Fig. 7 Schemes representing the adsorption of dye molecules on chitosan particles. Scheme I: Adsorption followed by the destruction of ionic crosslinking. Scheme II: Adsorption of dye followed by the adsorption on amino groups present in the dye molecules. The *dotted lines* represent electrostatic interactions

References

1. Kumar MNVR (2000) React Funct Polym 46:1
2. Constantine CA, Mello SV, Dupont A, Cao XH, Santos D, Oliveira ON, Strixino FT, Pereira EC, Cheng TC, Defrank JJ, Leblanc RM (2003) J Am Chem Soc 125:1805
3. dos Santos DS, Riul A, Malmegrim RR, Fonseca FJ, Oliveira ON, Mattoso LHC (2003) Macromol Biosci 3:591
4. Bengisu M, Yilmaz E (2002) Ceram Int 28:431
5. Pan JR, Huang C, Chen S, Chung YC (2000) Water Res 34:1057
6. Beppu MM, Arruda EJ, Vieira RS, Santos NN (2004) J Membr Sci 240:227
7. de Vasconcelos CL, Rocha ANL, Pereira MR, Fonseca JLC (2001) Polym Int 50:309
8. Rocha ANL, Fonseca JLC, Pereira MR (2002) J Appl Polym Sci 84:44
9. Khor E, Lim LY (2003) Biomaterials 24:2339
10. Mi FW, Tan YC, Liang HF, Sung HW (2002) Biomaterials 23:181
11. Hwang SM, Chen CY, Chen SS, Chen JC (2000) Biochem Biophys Res Commun 29:229
12. Suzuki T, Muzushima Y, Umeda T, Ohashi R (1999) J Ferment Bioeng 88:194
13. Shu XZ, Zhu KJ (2002) Eur J Pharm Biopharm 53:193
14. Shu XZ, Zhu KJ (2002) Eur J Pharm Biopharm 54:235
15. Ahn JS, Choi HK, Cho CS (2001) Biomaterials 22:923
16. Aral C, Akbuga J (1998) Int J Pharm 168:9
17. Aydin Z, Akbuga J (1996) Int J Pharm 131:101
18. Banerjee T, Mitra S, Singh AK, Sharma RK, Maitra A (2002) Int J Pharm 243:93
19. Berthold A, Cremer K, Kreuter J (1996) J Control Release 39:17
20. Lehr CM, Bouwstra JA, Schacht EH, Junginger HE (1992) Int J Pharm 78:43
21. Rayan P. A.and∼Pancholi V, Fischetti VA (2001) Infect Immun 69:7402
22. He P, Davis SS, Illum L (1998) Int J Pharm 166:75
23. Säkkinen M, Tuononen T, Jurjenson H, Jurjenson H, Veski P, Marvola M (2003) Eur J Pharm Sci 19:345
24. Marshall B (1983) Lancet 1:1273

25. Giunchedi P, Genta I, Conti B, Muzzarelli RAA, Conte U (1998) Biomaterials 19:157
26. Lorenzo-Lamosa ML, Remunan-Lopez C, Vila-Jato JL, Alonso MJ (1998) Biomaterials 52:109
27. van der Lubben IM, Verhoef JC, Borchard G (2001) Eur J Pharm Sci 14:201
28. Chiou MS, Li HY (2003) Chemosphere 50:1095
29. Gamzazade AI, Nasibov SM (2002) Carbohydr Polym 50:339
30. Chandy T, Sharma CP (1992) Biomaterials 13:949
31. Chandy T, Sharma CP (1993) Biomaterials 14:949
32. Gupta KC, Kumar MNVR (2000) Biomaterials 21:1115
33. Janes KA, Calvo P, Alonso MJ (2001) Adv Drug Deliver Rev 47:83
34. Ko JA, Park HJ, Hwang SJ, Park JB, Leen JS (2002) Int J Pharm 249:165
35. Denuziere A, Ferrier D, Domard A (1996) Carbohydr Polym 29:317
36. Hu Y, Jiang XQ, Ding Y, Ge HX, Yuan YY, Yang CZ (2002) Biomaterials 23:3193
37. Shiraishi S, Imai T, Otagiri M (1993) J Control Release 25:217
38. Sezer AD, Akbuga J (1995) Int J Pharm 121:113
39. Shu X, Zhu KJ (2000) Int J Pharm 201:51
40. de Campos AM, Sanchez A, Alonso MJ (2001) Int J Pharm 224:159
41. van der Lubben IM, Verhoef JC, van Aelst AC, Borchard G, Junginger HE (2001) Biomaterials 22:687
42. Hejazi R, Amiji M (2002) Int J Pharm 235:87
43. Bivas-Benita M, Laloup M, Versteyhe S, Dewit J, de Braekeleer J, Jongert E, Borchard G (2003) Int J Pharm 266:17
44. da Trindade Neto CG, Fernandes ALP, Santos AIB, Morais WA, Navarro MVM, Dantas TNC, Pereira MR, Fonseca JLC (2005) Polym Int 54:659
45. Prashanth KVH, Kittur FS, Tharanathan RN (2002) Carbohydr Polym 50:27
46. Taylor JR (1982) An introduction to error analysis, chap 3. University Science Books, Mill Valley, p 62
47. Chen YY, Oshima R, Uryu T, Kumanotani J (1985) Carbohydr Res 141:77
48. Thibault JF, Garreau C (1987) Carbohydr Res 163:15
49. da Trindade Neto CG, Pereira MR, Fonseca JLC (2002) Polym Degrad Stabil 76:227
50. de Vasconcelos CL, de Azevedo FG, Pereira MR, Fonseca JLC (2000) Carbohydr Polym 41:181
51. de Vasconcelos CL, Pereira MR, Fonseca JLC (2001) J Appl Polym Sci 80:1285
52. de Vasconcelos CL, de Medeiros DWO, de Moura KT, Acchar W, Dantas TNC, Pereira MR, Fonseca JLC (2003) Powder Technol 133:164
53. de Medeiros DWO, dos Santos DS, Dantas TNC, Pereira MR, Giacometti JA, Fonseca JLC (2003) Mater Sci Poland 21:251
54. Butterworth MD, Corradi R, Lascelles SF, Maeda S, Armes SP (1995) J Colloid Interf Sci 174:510
55. Sun T, Xu PX, Liu Q, Xue JA, Xie WM (2003) Eur Polym J 39:189
56. Peniche C, Elvira C, Roman JS (1998) Polymer 39:6549
57. Stoilova D, Wildner M, Koleva V (2002) J Mol Struct 643:37
58. Stoilova D, Lutz H (2002) J Mol Struct 606:267
59. Frost RL, Weier ML, Clissold ME, Williams PA (2003) Spectrochim Acta A 59:3313
60. Fernandes ALP, Martins RR, da Trindade Neto CG, Pereira MR, Fonseca JLC (2003) J Appl Polym Sci 89:191
61. de Vasconcelos CL, Martins RR, Ferreira MO, Pereira MR, Fonseca JLC (2002) Polym Int 51:69
62. Mao SR, Shuai XT, Unger F, Simon M, Bi DZ, Kissel T (2004) Int J Pharm 281:45
63. Missana T, Adell A (2000) J Colloid Interf Sci 230:150
64. de Vasconcelos CL, Dantas TN, Pereira MR, Fonseca JLC (2004) Colloid Polym Sci 282:596
65. Kiseleva MG, Radchenko LV, Nesterenko PN (2001) J Chromatogr A 920:79
66. Aksu Z (2001) Biochem Eng J 7:79
67. Chiou MS, Li HY (2002) J Hazard Mater 35:4169
68. Juang RS, Tseng RL, Wu FC, Lee SH (1997) J Chem Technol 70:391
69. Wu FC, Tseng RL, Juang RS (2000) J Hazard Mater B73:63